Curie temperatures of III–V diluted magnetic semiconductors calculated from first principles

2003 Europhys. Lett. 61 403

(http://iopscience.iop.org/0295-5075/61/3/403)

EUROPHYSICS LETTERS 1 February 2003

Europhys. Lett., **61** (3), pp. 403–408 (2003)

Curie temperatures of III-V diluted magnetic semiconductors calculated from first principles

K. SATO[1,2], P. H. DEDERICS[1] and H. KATAYAMA-YOSHIDA[2]

[1] *Institut für Festkörperforschung, Forschungszentrum Jülich*
D-52425 Jülich, Germany
[2] *Department of Condensed Matter Physics*
The Institute of Scientific and Industrial Research (ISIR), Osaka University
8-1 Mihogaoka, Ibaraki, Osaka 567-0047, Japan

(received 12 August 2002; accepted 25 November 2002)

PACS. 75.50.Pp – Magnetic semiconductors.

Abstract. – Curie temperatures of the diluted magnetic semiconductors (Ga, Mn)As, (Ga, Mn)N, (Ga, Cr)As and (Ga, Cr)N are evaluated from first principles. The electronic structure is calculated in the local spin density approximation by using the Korringa-Kohn-Rostoker method combined with the coherent potential approximation to describe the substitutional and spin disorder. From the total energy differences between the ferromagnetic state and the spin-glass state, realistic estimations of Curie temperatures are achieved by using a mapping on the Heisenberg model in the mean-field approximation. Effects of additional carrier doping treatments are also investigated. Very large Curie temperatures are obtained, lying above room temperature for (Ga, Mn)N, (Ga, Cr)As and (Ga, Cr)N. Upon hole doping the Curie temperature of (Ga, Mn)N further increases, while (Ga, Mn)As shows a plateau behavior.

The recent discovery of the carrier-induced ferromagnetism in (In, Mn)As [1] and (Ga, Mn)As [2] encourages many experimental and theoretical studies on diluted magnetic semiconductors (DMS), because DMS are candidates for new functional materials whose magnetic properties are controllable by changing the carrier density. These new materials are believed to be a fundamental element to establish a spin-based electronics (Spintronics) as a practical technology [3]. From the application point of view, the low Curie temperatures (T_C) of the investigated DMS represent a serious problem, and many efforts have been devoted to find ferromagnetic DMS with T_C higher than room temperature. To predict DMS with high T_C is still a challenging task for theory, because the underlying mechanism of their ferromagnetism has not been completely understood. Recently, Dietl *et al.* proposed Zener's *p-d* exchange model to describe the carrier-induced ferromagnetism and predicted some high-T_C DMS based on a mean-field theory [4]. The ferromagnetism in a quantum well structure of DMS was also investigated based on a mean-field theory [5]. Recent reviews for theories on the ferromagnetism in DMS are found in refs. [5] and [6].

In this letter, instead of starting from a model Hamiltonian, we take a different approach to describe DMS, *i.e.*, first-principles electronic structure calculations based on density functional theory. For the purpose of describing the overall trend in the magnetism of DMS, first-principles calculations represent a powerful and efficient tool, because they do not need any parameters obtained from experiments. The electronic structures of DMS are calculated based on the local spin density approximation (LSDA). In DMS, transition metal impurities

(TM) are introduced randomly into cation sites of the host semiconductor. This substitutional disorder in DMS is well described by the Korringa-Kohn-Rostoker coherent-potential approximation (KKR-CPA) method [7]. In the CPA, configuration-averaged properties of alloys are calculated within a single-site approximation, therefore we can simulate arbitrary concentrations of impurities without using a large artificial supercell. By this method, it is also possible to take magnetic disorder into account [8, 9]. We can simulate the spin-glass (or "disordered local moment") state with a vanishing total moment by considering a multi-component alloy consisting of $TM^{\uparrow}$, $TM^{\downarrow}$ and host atoms at the cation site, where up and down arrows indicate the direction of the local moment of the TM impurity. As a consequence, in the single-site approximation calculations for non-collinear states are not required. While this method is well suited for the metallic phase in the experimentally interesting concentration region, it cannot describe the Motto insulator or Anderson localisation transition to the insulating spin-glass state at very low concentrations. It is known that this approach gives a good description of the paramagnetic state of ferromagnets above T_{C} [10–12]. In this letter, III-V compound-based DMS of (Ga, TM)Y, where TM refers to Mn or Cr impurities and Y to As or N anions, are discussed as typical examples.

In order to discuss the ferromagnetism of DMS, the total energies (TE's) of both the ferromagnetic state, described as $(\mathrm{Ga}_{1-x},\ \mathrm{TM}_{x}^{\uparrow})\mathrm{Y}$, and the spin-glass state, described as $(\mathrm{Ga}_{1-x},\ \mathrm{TM}_{x/2}^{\uparrow},\ \mathrm{TM}_{x/2}^{\downarrow})\mathrm{Y}$, are calculated and in particular the energy difference $\Delta E = TE(\text{spin-glass state}) - TE(\text{ferromagnetic state})$ is estimated. Throughout the present calculations, we used the KKR-CPA package (MACHIKANEYAMA2000) developed by Akai [13]. The shape of the crystal potential is approximated by a muffin-tin potential, and the wave functions are calculated up to $l = 2$, where l is the angular momentum quantum number defined at each atomic site. Local lattice distortions are neglected and the experimental lattice constants of pure GaN ($a = 3.180\,\text{Å}$, $c = 5.166\,\text{Å}$ and $u = 0.377$; wurtzite structure) and pure GaAs ($a = 5.6537\,\text{Å}$; zinc blende structure) are used in the calculations [14]. For GaN-based DMS, 105 k-points in the irreducible part of the first Brillouin zone are used in the calculations, while for GaAs-based DMS, 195 k-points are used. Relativistic effects are considered in the scalar relativistic approximation.

Since the LSDA describes only the ground-state properties, we need an additional procedure to estimate T_{C}. To describe the magnetic properties at finite temperatures we use the Heisenberg model, which can be written as $H = -\Sigma_{i \neq j} J_{ij} \vec{S}_i \vec{S}_j$, where $\vec{S}_i$ is the spin at site i and J_{ij} is the exchange coupling constant between sites i and j. We can calculate the total energy difference ΔE^{H} in this Heisenberg model within the mean-field approximation as $\Delta E^{\mathrm{H}} = S^2 c^2 \Sigma_{n \neq 0} J_{n0}$, where c is the concentration of the magnetic ions and n sums over all sites of the cation sublattice. This ΔE^{H} can be directly identified with the energy difference ΔE calculated from first principles, since the CPA represents also a mean-field theory. On the other hand, within the mean-field theory of the Heisenberg model we can estimate T_{C} by using the Brillouin function expression, known as the molecular field theory, leading to $k_{\mathrm{B}} T_{\mathrm{C}} = \frac{2}{3} S^2 c \Sigma_{n \neq 0} J_{n0}$, where k_{B} is the Boltzmann constant. The result $k_{\mathrm{B}} T_{\mathrm{C}} = \frac{2}{3} \Delta E / c$ allows to evaluate T_{C} from first principles.

Figure 1 shows the Curie temperatures of (Ga, Mn)As, (Ga, Mn)N, (Ga, Cr)As and (Ga, Cr)N calculated in this way. As is shown in the figure, for lower concentrations the T_{C}'s fastly increase, approximately proportional to the square root of concentration of TM impurities, but saturate more or less for higher concentrations. For all compounds, room temperature ferromagnetism is predicted in realistic concentration ranges. In particular, it is found that the Curie temperatures go up to 600 K in Cr-doped GaN and GaAs. For 5% Mn-doped GaAs, T_{C} is calculated as 260 K, which is much higher than the experimental value

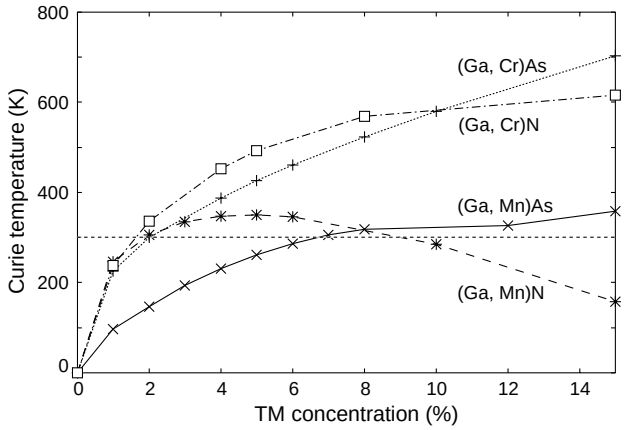

Fig. 1 – Curie temperatures of (Ga, Mn)As, (Ga, Mn)N, (Ga, Cr)As and (Ga, Cr)N calculated from first principles. The dashed horizontal line indicates room temperature (300 K).

of 110 K [15]. However, when comparing with experiment one has to remember that the mean-field approximation usually somewhat overestimates the Curie temperature of ferromagnets, which is in our case presumably not a large effect due to the long-range nature of the interaction. Moreover, due to compensation effects the effective Mn concentration is not well known. In the present calculation the neutral solution of the impurity problem is considered, *i.e.*, the impurity bands are occupied with 4 electrons per Mn atom, 3 electrons per Cr atom, respectively. Effects of additional carrier doping will be discussed later. In case of (Ga, Mn)N, we have a maximum T_{C} of approximately 350 K, which seems to be inconsistent with recent experimental T_{C} of 940 K [16]. Recently, Cr-doped GaN was synthesized and reported to have T_{C} higher than 400 K for several percent of Cr impurities [17]. This experimental result seems to be consistent with our calculations.

In order to discuss the origin of the ferromagnetism, the density of states (DOS) is calculated. The total DOS per unit cell and the partial density of d-states at each TM impurities are shown in fig. 2. As shown in the figure, all of them show a half-metallic DOS, therefore the total magnetic moments of Cr-doped and Mn-doped systems scale with the impurity concentration, with the proportionality factor being $3.0\mu_{\mathrm{B}}$ per Cr impurity and $4.0\mu_{\mathrm{B}}$ per Mn impurity. The impurity states, which are basically anti-bonding states originating from the hybridization between impurity-$d\epsilon$ states and the host valence band, appear in the band gap [18]. As is discussed in ref. [19], the wave functions of these gap states can be considered as evanescent bulk states, the decay parameters of which are determined by the host complex band structure. If their tails are sufficiently long, a certain overlap of the impurity wave functions is expected leading to impurity bands. It is this long-range interaction which explains the occurrence of ferromagnetism in these diluted systems. In fact, the calculated DOS show impurity bands for (Ga, Mn)N, (Ga, Cr)As and (Ga, Cr)N in the band gap region as shown in fig. 2(b), (c) and (d), respectively. In these cases, it is very likely that the ferromagnetism originates from Zener's double-exchange mechanism as has already been pointed out by Akai [9]. This picture also allows us to understand the $\sqrt{c}$-dependence of the calculated Curie temperature. The stability of the ferromagnetic state scales as the half-width of the impurity band. However, in general the band width is proportional to the square root of the effective coordination number, and in a mean-field approximation this number increases linearly with the concentration c. In fact, our CPA calculations confirm the $\sqrt{c}$-dependence of the impurity

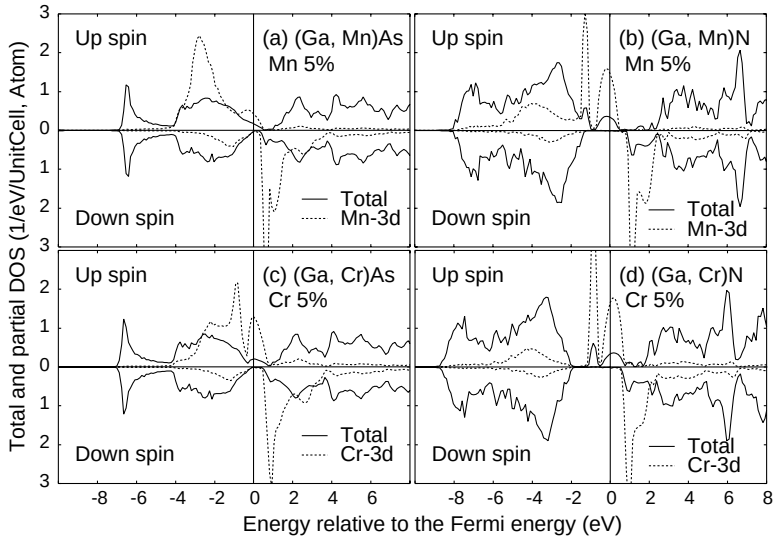

Fig. 2 – Total density of states per unit cell (solid line) and partial density of $3d$ states at TM site per atom (dotted line) in (a) (Ga, Mn)As, (b) (Ga, Mn)N, (c) (Ga, Cr)As and (d) (Ga, Cr)N in the ferromagnetic states. TM impurities are doped up to 5%, respectively. The horizontal axis denotes the energy relative to the Fermi energy.

band half-widths. In case of (Ga, Mn)As, the impurity states merge together with the host valence bands and the peak structure is less pronounced. Therefore, it is difficult to say which electrons take part in the ferromagnetism. However, states at the Fermi level (E_{F}) still have a large amplitude of d states as shown in fig. 2(a), so the double-exchange picture is still valid.

Next, the effect of additional carrier doping is investigated in (Ga, Mn)N and (Ga, Mn)As. Hole carriers are introduced by substitutional Mg impurities on Ga sites in both compounds.

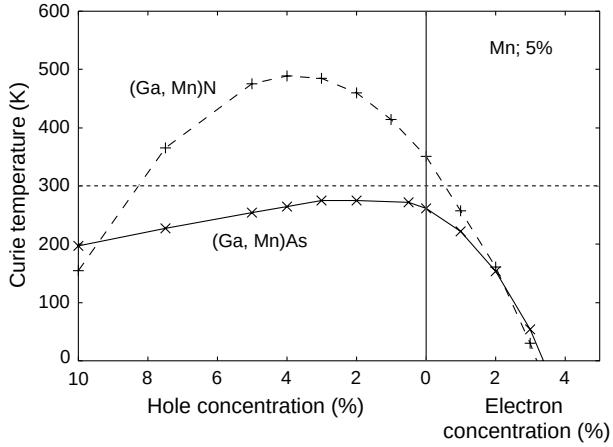

Fig. 3 – Curie temperatures of (Ga, Mn)N and (Ga, Mn)As as a function of additional carrier concentration. Hole carriers are doped by substituting Ga by Mg for both DMS. Electrons are doped by O and As introduced at N and Ga site for (Ga, Mn)N and (Ga, Mn)As, respectively.

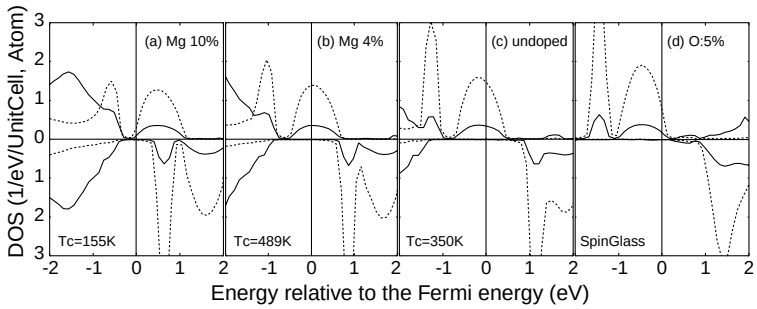

Fig. 4 – Total DOS per unit cell (solid lines) and partial density of Mn-d states per Mn atom (dotted lines) in ferromagnetic (Ga, Mn)N. (a) Mg: 10%, (b) Mg: 4% and (d) O: 5% are additionally introduced into (Ga, Mn)N. In (c), no additional carrier doping treatment is performed.

Electrons are introduced by substituting N by O in (Ga, Mn)N. For electron doping into (Ga, Mn)As, we take anti-site As atoms which behave as double donors in GaAs. The difference between single and double donors has already been studied in ref. [9]. The calculated T_{C}'s are shown in fig. 3 as a function of additional hole and electron concentrations. Both for (Ga, Mn)N and for (Ga, Mn)As, the T_{C}'s break down sharply with increasing electron concentrations and above 3% the ferromagnetism disappears. This response to electron doping is very consistent with the experimental evidence, and experimental T_{C} values for (Ga, Mn)As are consistent with our first-principles calculations if compensation is taken into account [15]. As shown in fig. 3, it is found that hole doping into (Ga, Mn)N can dramatically enhance T_{C}, which goes up to about 500 K for 4% hole doping. However, this value is still too low to explain the recently reported $T_{\mathrm{C}} = 940\,\mathrm{K}$ [16].

The dependence of T_{C} of (Ga, Mn)N on carrier concentration is easily understood by analysing the DOS. Figure 4 shows calculated total and partial DOS of (Ga, Mn)N for various additional carrier concentrations. In all cases, the DOS of the ferromagnetic states is plotted. According to the double-exchange picture, the ferromagnetic interaction originates from the kinetic-energy gain of itinerant d-electrons. This means that the ferromagnetism is most stable when E_{F} is located at the center of the impurity band and the DOS at E_{F} is highest. Without additional carriers, E_{F} is located at the higher energy side of the impurity peak as shown in fig. 4(c). With increasing hole concentration, E_{F} is shifted to lower energy. As a result, E_{F} approaches the peak of the DOS and simultaneously T_{C} reaches a maximum (fig. 4(b)). Taking into account that this impurity band accommodates 3 electrons in total, T_{C} should be maximal for 2.5% of additional holes, while in fact the calculation gives a maximum for about 4% of additional holes (see fig. 3). At higher hole concentrations, E_{F} overtakes the peak of DOS, and the impurity band becomes completely empty for a 10% hole concentration (fig. 4(a)). As a result, T_{C} goes down. As shown in fig. 4(d), a 5% electron doping compensates almost all hole states, and the ferromagnetic state is no longer stable.

In contrast to (Ga, Mn)N, the (Ga, Mn)As system is remarkably insensitive to hole doping as is shown in fig. 3. Here the Mn-d states strongly hybridize with GaAs valence band (fig. 2(a)). Therefore, the impurity peak is very broad and merges with the valence band so that the doped holes occupy not only impurity states but also host valence states. As a result, (Ga, Mn)As is less sensitive to hole doping as compared to (Ga, Mn)N. Nevertheless, hole doping into (Ga, Mn)As is a good strategy to realize high T_{C}, because it is experimentally known that hole states originating from Mn impurities are usually compensated in (Ga, Mn)As by anti-site As [15].

In summary, we have investigated the electronic structure of III-V compound-based DMS and estimated their Curie temperatures from first-principles KKR-CPA calculations combined with the Heisenberg model within the mean-field approximation. According to our results, it is possible to build room temperature ferromagnets with the compounds investigated in this letter. In particular, Cr-doped GaN and GaAs are good candidates for high-T_C ferromagnets. The effects of additional carrier doping are also investigated. It is shown that the ferromagnetism becomes unstable by the compensation of hole states in (Ga, Mn)N and (Ga, Mn)As. However, by hole doping it is possible to increase T_C of (Ga, Mn)N substantially, while on the other hand T_C of (Ga, Mn)As is insensitive to hole doping. The calculated DOS strongly suggests that the impurity band formed in the band gap is responsible for the ferromagnetism in DMS. This evidence strongly supports Zener's double-exchange picture as the origin of ferromagnetism.

* * *

This research was partially supported by JSPS Research for the Future Program in the Area of Atomic-Scale Surface and Interface Dynamics, a Grant-in-Aid for Scientific Research on Priority Areas (A) and (B), and SANKEN-COE from the Ministry of Education and Science, Sports and Culture. One of the authors (KS) acknowledges financial support to JSPS. This work was also partially supported by the RT Network Computational Magnetoelectronics (Contract RTN1-1999-00145) of the European Commission.

REFERENCES

[1] Ohno H., Munekata H., Penney T., von Molnár S. and Chang L. L., *Phys. Rev. Lett.*, **68** (1992) 2664.
[2] Ohno H., Shen A., Matsukura F., Oiwa A., Endo A., Katsumoto S. and Iye Y., *Appl. Phys. Lett.*, **69** (1996) 363.
[3] Wolf S. A., Awschalom D. D., Buhrman R. A., Daughton J. M., von Molnár S., Roukes M. L., Chtchelkanova A. Y. and Treger D. M., *Science*, **294** (2001) 1488.
[4] Dietl T., Ohno H., Matsukura F., Civert J. and Ferrand D., *Science*, **287** (2000) 1019.
[5] Lee B., Jungwirth T. and MacDonald A. H., *Semicond. Sci. Technol.*, **17** (2002) 393.
[6] Dietl T., *Semicond. Sci. Technol.*, **17** (2002) 377.
[7] Akai H., *J. Phys. Condens. Matter*, **1** (1989) 8045.
[8] Akai H. and Dederichs P. H., *Phys. Rev. B*, **47** (1993) 8739.
[9] Akai H., *Phys. Rev. Lett.*, **81** (1998) 3002.
[10] Oguchi T., Terakura K. and Hamada N., *J. Phys. F*, **13** (1983) 145.
[11] Gyorffy B. L., Pindor A. J., Staunton J., Stocks G. M. and Winter H., *J. Phys. F*, **15** (1985) 1337.
[12] Staunton J., Gyorffy B. L., Pindor A. J., Stocks G. M. and Winter H., *J. Phys. F*, **15** (1985) 1387.
[13] Akai H., Department of Physics, Graduate School of Science, Osaka University, Machikaneyama 1-1, Toyonaka 560-0043, Japan; `akai@phys.sci.osaka-u.ac.jp` (2000).
[14] Wyckoff R. W. G., *Crystal Structures* (Wiley, New York) 1986, p. 108.
[15] Matsukura F., Ohno H., Shen A. and Sugawara Y., *Phys. Rev. B*, **57** (1998) R2037.
[16] Sonoda S., Shimizu S., Sasaki T., Yamamoto Y. and Hori H., *J. Cryst. Growth*, **237-239** (2002) 1358.
[17] Hashimoto M., Zhou Y. K., Kanamura M. and Asahi H., *Solid State Commun.*, **37** (2002) 122.
[18] Sato K. and Katayama-Yoshida H., *Semicond. Sci. Technol.*, **17** (2002) 367.
[19] Mavropoulos Ph., Papanikolaou N. and Dederichs P. H., *Phys. Rev. Lett.*, **85** (2000) 1088.